EUROPEAN JOURNAL OF PURE AND APPLIED MATHEMATICS
2026, Vol. 19, Issue 2, Article Number 7256
ISSN 1307-5543 – ejpam.com
Published by New York Business Global

Mathematical Analysis of Monkeypox Disease Using Fractional Delay Differential Equations and Vaccination Control

Jatin Bansal[1], Anoop Kumar[1,*], Aziz Khan[2], Khaled Naseralla[3], Thabet Abdeljawad[2,4,5], Rajermani Thinakaran[6]

[1] *Department of Mathematics and Statistics, Central University of Punjab, 151401-Bathinda, Punjab, India*
[2] *Department of Mathematics and Science, Prince Sultan University, 11586-Riyadh, Saudi Arabia*
[3] *Preparatory Year Program, Colllege of Humanities and Sciences, Prince Sultan University, 11586-Riyadh, Saudi Arabia*
[4] *Department of Fundamental Sciences, Faculty of Engineering and Architecture, Istanbul Gelisim University, Avcılar- Istanbul, 34310, Türkiye*
[5] *Department of Mathematics and Applied Mathematics, Sefako Makgatho Health Sciences University, Garankuwa, Medusa 0204, South Africa*
[6] *Faculty of Data Science and Information Technology, INTI International University, Negeri Sembilan, Malaysia*

Abstract. This study presents a fractional-order model for the transmission dynamics of Monkeypox, formulated using Caputo fractional order delay differential equations. The model incorporates two types of delays: one representing diagnostic delays in humans and the other associated with rodent populations. The proposed framework further integrates vaccination strategies and assesses the demand for clinical care. Analytically, the existence, uniqueness, non-negativity, and boundedness of solutions have been established. The basic reproduction number R_0 has been derived, and a sensitivity analysis identifies the parameters most influencing R_0. Specifically, the transmission rates β_1 and β_3, and the parameter ω_1 exhibit the strongest influence, whereas the γ has the least impact. Furthermore, the stability of the disease-free and endemic equilibria has been investigated using the curve-switching method in the presence of time delays. Additionally, graphical simulations demonstrated the effects of delays, vaccination rates, and fractional orders. The results indicate that increasing the vaccination rate reduces the infected population, and large values of the delay parameters of the model produce slower disease trajectories and lower infection peaks at fixed time as compared to delays with lower values. This reflects a slower system response rather than the actual situation. These findings highlight the sensitivity of disease progression to delays.
2020 Mathematics Subject Classifications: 26A33, 34A08, 37M05, 37N25, 47H10, 93C43.
Key Words and Phrases: Monkeypox, caputo derivative, sensitivity analysis, stability analysis, delay differential equation, predictor-corrector method.

*Corresponding Author.
DOI: https://doi.org/10.29020/nybg.ejpam.v19i2.7256

Email addresses: jatin96bansal@gmail.com (B. Jatin), anoop.kumar@cup.edu.in (K. Anoop)

1. Introduction

Monkeypox (also known as Mpox [1]) is a viral zoonotic disease belonging to the poxviridae family's orthopoxvirus genus. This family includes Smallpox, Variola, and Cowpox viruses. Monkeypox has symptoms similar to those seen in human smallpox patients. After the eradication of smallpox, monkeypox became the most common orthopox virus, as a result on 14 August 2024, WHO Director-General Dr. Tedros Adanom declared Mpox a Public health emergency of International Concern [2]. The initial case of Mpox was documented in a Cynomolgus monkey in 1959, hence causing the disease to be known as Monkeypox [3]. During the 1960s, there were four animal outbreaks of Mpox, but no human cases were reported [4–6]. In 1970, a 9-month-old infant was believed to have been the first human victim of Mpox in the Democratic Republic of the Congo [7]. According to a study conducted on [8], 155 instances of Mpox in West and Central Africa between 1970 and 1983, interaction with monkeys and squirrels was thought to have caused merely 20 percent of the cases. It was observed that the human-to-human transmission ceased on its own, and the incident rates among families without a smallpox vaccination were estimated to be 15%, while the vaccination rate was 0.4%. The global commission has opted to discontinue smallpox vaccination efforts in Central African countries where Mpox is regarded as endemic. This decision is grounded in the low attack rates of the disease and the consistent secondary attack rates observed among unvaccinated individuals during the 1970s and early 1980s [9].

In most instances, monkeypox is a self-limiting illness that persists for two to four weeks [10]. In children, expectant mothers, or people with impaired immunity from other medical issues, it may be more severe. The period of incubation may span anywhere from 5 to 21 days, which generally spans 6 to 13 days [11]. The common symptoms of Mpox include rash, fever, sore throat, headache, muscle aches, back pain, low energy, and swollen lymph nodes [12]. Individuals with monkeypox can transmit the virus to others until all sores have healed and new skin has formed. Some people may be infected without displaying any symptoms. Although there have been reports of people getting monkeypox from someone who is asymptomatic, information on how common this is remains limited. Monkeypox spreads mainly through close contact with an infected person. Additionally, human-to-animal transmission can occur through bites or scratches from infected animals. The source of the monkeypox virus is currently unknown, and ongoing studies are being conducted to determine it.

As of the 1st January 2022, cases have been reported to WHO from 116 Member States across all 6 WHO regions [13]. As of 30 June 2024, 99176 laboratory-confirmed cases had been reported to WHO, with 208 deaths. The monthly reported new cases in August 2024 [14] surged by 15.6% as compared to previous month. The majority of cases reported during the previous month originated in African (62.3%) and European (13.7%) regions. The 10 most affected countries globally, as of 1 January 2022, are: United States of America (n = 33812), Brazil (n = 12206), Spain (n = 8240), Democratic Republic of the Congo (n = 6092), France (n =4307), Colombia (n =4262), Mexico (n = 3909). Together, these countries account for 79.9% of the cases reported globally.

The most useful laboratory test is the identification of viral DNA using polymerase chain reaction (PCR) for Mpox [15]. Optimal diagnostic specimens are collected from the rash skin, and crusts or fluid after vigorous swabbing. If there are no skin lesions, swabs of the throat or anus can be performed for testing. Blood tests for Mpox detection are not advised since antibody detection techniques are ineffective at differentiating between orthopoxviruses. Most Mpox cases are resolved with supportive care; only a small percentage of patients require clinical Mpox treatment, which involves providing patients with antiviral drugs. The first is Tecovirimat 600 mg oral medication, which is used twice daily for 14 days. It was approved for Mpox by the FDA (Food and Drug Administration) in July 2018. Second is Brincidofovir 200 mg oral route, which requires two weekly treatments and has FDA approval for Mpox in June 2021. Some patients also take Cidofovir, which has side effects linked to the kidneys and is not approved by the FDA. Additionally, the WHO began an Mpox immunization campaign [16] using the following three vaccinations: MVA-BN, LC16m8, and ACAM2000.

Researchers have developed various mathematical models for monkeypox based on recent biological research and outbreak data [17–20]. One novel deterministic model revealed that isolating infected individuals can reduce disease incidence [21–24]. Several studies have examined the various ways that monkeypox is transmitted using nonlinear differential equations, showing that an individual's immunological status affects their recovery from the infection [25–29]. Several epidemic models have been investigated to understand transmission mechanisms and control methods [30–33].

The fractional-order derivative is employed to incorporate memory and hereditary properties of the disease process. In the context of monkeypox, diagnostic delays, immunity development, and recurrent exposures make the current state of the system dependent not only on present conditions but also on past interactions. The order α in the Caputo derivative thus acts as a measure of this memory: values of $\alpha < 1$ indicate memory effects. In the existing literature, several studies have investigated the transmission dynamics of Mpox [22, 34–36], yet a significant gap remains regarding the incorporation of time delays. According to the World Health Organization (WHO) report [14], there is typically a diagnostic delay of approximately 7–14 days in confirmed Mpox cases. Motivated by this observation, we incorporate time delays into the proposed model: one delay representing diagnostic delays in humans and a second delay associated with the rodent population.

The incorporation of delay as an equation of fractional differential into epidemic modeling is a significant advancement, as it accounts for the inherent duration of delays in disease communication and preventive actions, this includes factors such as lack of laboratory, incubation periods, and the duration for interventions to take effect. By integrating delays, one can precisely forecast disease situation and evaluate the significance of preventive techniques. It signifies the need for research articles utilizing delay differential equations related to monkeypox and its latent period. Therefore, a mathematical dynamical system is required to account for the disease's history, using delay equations to reflect the latent period in humans and rodents.

The structure of the paper is as follows: The "Preliminaries" section provides essential definitions and concepts related to the purpose model. The "Mathematical model" section

details the formulation of the model along with the underlying assumptions. The "Main Results" section presents the analytical findings, including the existence and uniqueness of the model's solution, non-negativity and boundedness, equilibrium points, the basic reproduction number, sensitivity analysis, and stability analysis employing using switching curve technique. The "Numerical Simulations" section describes the MATLAB-based experiments that illustrate the effects of delays, vaccination and fractional order on the system dynamics. Lastly, the "Conclusion" section summarizes the principal findings and discusses their implications for Mpox outbreaks.

2. Preliminaries results

Fractional differential operators are crucial in mathematical modeling and have proven effective in numerous fields, including science, engineering, and epidemiology. This study outlines the essential definitions and properties utilized throughout the research.

Definition 1. *[37] The Caputo fractional derivative operator of the function* $\Delta \in \mathbb{C}^0[0,T]$ *is;*

$$ {}^{C}D_t^{\alpha}\Delta(t) = \frac{1}{\Gamma(m-\alpha)}\int_0^t \frac{\Delta^{(m)}(\tau)d\tau}{(t-\tau)^{\alpha+1-m}}, $$

where $m = \lfloor \alpha + 1 \rfloor$ *and* $\lfloor \alpha \rfloor$ *represent an integral part of* α*.*

Proposition 1. *[38] Laplace transform of Caputo's derivative of order* α *is given by;*

$$ L\{{}^{C}D_t^{\alpha} f(t); s\} = s^{\alpha}F(s) - \sum_{k=0}^{n-1} s^{\alpha-k-1} f^k(0), \qquad n-1 \leq \alpha < n. $$

3. Mathematical model

In this paper, we investigate the transmission dynamics of Mpox in both human and rodent populations. The total human population (N_h) is subdivided into six compartments: susceptible (S_h), exposed (E_h), infected (I_h), clinically ill (C_h), vaccinated (V_h), and recovered (R_h) individuals at time t. Similarly, the rodent population (N_r) is partitioned into three classes: susceptible (S_r), infected (I_r), and recovered (R_r) at time t. A schematic representation of the model is presented in flowchart. The proposed model is formulated under the following assumptions:

1. The constant rate of natural death is ν_h, while the rate at which susceptible people are born is Δ_1. α_h is the constant vaccination rate of susceptible.

2. The class of exposed individuals is increased by joining the newly infected individuals with the force of infection $\delta_h = \left(\beta_1 \frac{I_h}{N_h} + \beta_2 \frac{I_r}{N_r}\right)$ where β_1 and β_2 are the rate of which population becoming infected as a result of contact with animals and people who are infected.

Parameter	Value	Source	Parameter	Value	Source
Δ_1	0.169	[39]	μ_h	0.2393	[23]
Δ_2	2	[40]	ν_h	0.086	[39]
ς	0.9894	[19]	ϑ_1	0.00217	[13]
γ	0.0019	[23]	w_1	0.4670	[23]
β_3	0.0486	[23]	ϑ_2	0.1	[23]
β_1	0.5701	[23]	ϑ_3	0.4	[40]
ν_r	1.5	[40]	w_2	0.83	[40]
β_2	0.00252	[19]			

Table 1: Parameters value with sources

3. If τ_1 represent the latent period of human to human disease i.e. time taken by susceptible individuals to become infectious is τ_1, hence after taking into consideration deaths of exposed individuals in the period of latency, the number of human entering infectious class come out be $\delta_h^{'} = \left(\beta_1^{'} \frac{I_h(t-\tau_1)}{N_h(t-\tau_1)} + \beta_2^{'} \frac{I_r(t-\tau_1)}{N_r(t-\tau_1)}\right)$, where $\beta_1^{'}$ and $\beta_2^{'}$ are equal to $\beta_1 e^{-\nu_h \tau_1}$ and $\beta_2 e^{-\nu_h \tau_1}$ respectively.

4. Let γ is the rate at which human get infected class to clinically ill class with ς as rate of recovery of clinical ill humans. ϑ_2 is the death rate of clinically ill humans. w_1 is the recovery rate in humans due to immunity and ϑ_1 is the disease induced death rate in humans.

5. Natural rate of death in rodents represented by ν_r and susceptible rodents born rate is Δ_2.

6. The reduction rate in the class of susceptible rodents is $\delta_r = \left(\frac{\beta_3 I_r}{N_r}\right)$, where β_3 represents rate at which disease transmitted among rodents.

7. τ_2 represent the incubation period of rodents i.e. time taken by rodents to show infection so number of rodents entering infection class at the rate $\left(\frac{\beta_3^{'} I_r(t-\tau_2)}{N_r(t-\tau_2)}\right)$, where $\beta_3^{'} = \beta_3 e^{-\nu_r \tau_1}$.

8. w_2 and ϑ_3 are the recovery rates due to immunity of non humans and disease induced morality rate of infected animals.

After taking into account all of the presumptions, the models' mathematical structure is;

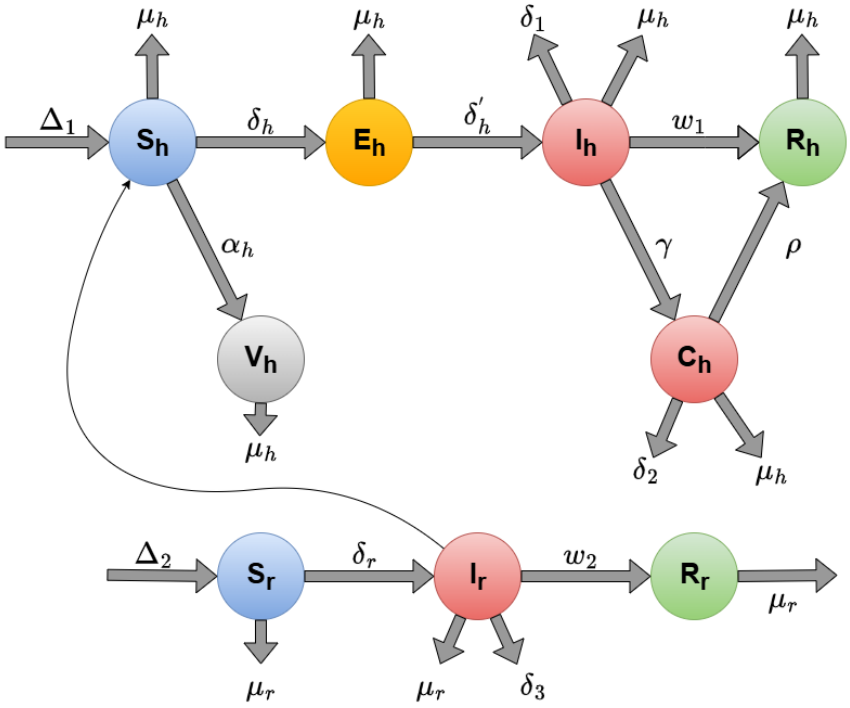

Figure 1: Flowchart of Mpox transmission

$$
\begin{aligned}
D_t^\alpha S_h &= \Delta_1 - \left(\beta_1 \frac{I_h}{N_h} + \beta_2 \frac{I_r}{N_r}\right) S_h - (\nu_h + \mu_h) S_h, \\
D_t^\alpha E_h &= \left(\beta_1 \frac{I_h}{N_h} + \beta_2 \frac{I_r}{N_r}\right) S_h - \left(\beta_1' \frac{I_h(t-\tau_1)}{N_h(t-\tau_1)} + \beta_2' \frac{I_r(t-\tau_1)}{N_r(t-\tau_1)}\right) S_h(t-\tau_1) - \nu_h E_h, \\
D_t^\alpha I_h &= \left(\beta_1' \frac{I_h(t-\tau_1)}{N_h(t-\tau_1)} + \beta_2' \frac{I_r(t-\tau_1)}{N_r(t-\tau_1)}\right) S_h(t-\tau_1) - (w_1 + \gamma + \nu_h + \vartheta_1) I_h, \\
D_t^\alpha C_h &= \gamma I_h - (\varsigma + \nu_h + \vartheta_2) C_h, \\
D_t^\alpha V_h &= \mu_h S_h - \nu_h V_h, \\
D_t^\alpha R_h &= \varsigma C_h + w_1 I_h - \nu_h R_h, \\
D_t^\alpha S_r &= \Delta_2 - \left(\frac{\beta_3 I_r}{N_r}\right) S_r - \nu_r S_r, \\
D_t^\alpha I_r &= \left(\frac{\beta_3' I_r(t-\tau_2)}{N_r(t-\tau_2)}\right) S_r(t-\tau_2) - (w_2 + \nu_r + \vartheta_3) I_r, \\
D_t^\alpha R_r &= w_2 I_r - \nu_r R_r.
\end{aligned}
\tag{1}
$$

Under the initial condition

$$\begin{aligned}
&\tau_1 > 0, \quad \tau_2 > 0,\\
&S_h(\theta) = \varphi_1(\theta), \quad E_h(0) \geq 0, \quad I_h(\theta) = \varphi_2(\theta), \quad C_h(0) \geq 0, \quad V_h(0) \geq 0, \quad R_h(0) \geq 0, \\
&S_r\theta = \varphi_3(\theta), \quad I_r(\theta) = \varphi_4(\theta), \quad R_r(0) \geq 0, \quad (-\tau_1, \tau_2 \leq \theta \leq 0).
\end{aligned} \tag{2}$$

Where $\varphi = (\varphi_1, E_h(0), \varphi_2, C_h(0), V_h(0), R_h(0), \varphi_3, \varphi_4, R_r(0))^T \in \mathfrak{C}.\mathfrak{C}([-\tau, 0], \mathbb{R}^9_+)$ is continuous mapping Banach space on $[-\tau, 0]$ to $\mathbb{R}^9_+$.

Since $E_h(t)$ is not contained in further equations, we can amend our mathematical framework as follows;

$$\begin{aligned}
D_t^\alpha S_h &= \Delta_1 - \left(\beta_1 \frac{I_h}{N_h} + \beta_2 \frac{I_r}{N_r}\right) S_h - (\nu_h + \mu_h) S_h,\\
D_t^\alpha I_h &= \left(\beta_1' \frac{I_h(t-\tau_1)}{N_h(t-\tau_1)} + \beta_2' \frac{I_r(t-\tau_1)}{N_r(t-\tau_1)}\right) S_h(t-\tau_1) - (w_1 + \gamma + \nu_h + \vartheta_1) I_h,\\
D_t^\alpha C_h &= \gamma I_h - (\varsigma + \nu_h + \vartheta_2) C_h,\\
D_t^\alpha V_h &= \mu_h S_h - \nu_h V_h,\\
D_t^\alpha R_h &= \varsigma C_h + w_1 I_h - \nu_h R_h,\\
D_t^\alpha S_r &= \Delta_2 - \left(\frac{\beta_3 I_r}{N_r}\right) S_r - \nu_r S_r,\\
D_t^\alpha I_r &= \left(\frac{\beta_3' I_r(t-\tau_2)}{N_r(t-\tau_2)}\right) S_r(t-\tau_2) - (w_2 + \nu_r + \vartheta_3) I_r,\\
D_t^\alpha R_r &= w_2 I_r - \nu_r R_r,
\end{aligned} \tag{3}$$

with the same initial conditions (2).

4. Main work

4.1. Existence and uniqueness of the solution

Writing system (3) as follows will demonstrate both the solution's existence and uniqueness;

$$\begin{aligned}
&D_t^\alpha Y(t) = X(t, Y(t), Y(t-\tau)),\\
&Y(0) = \varphi, \quad -\tau \leq t \leq \Im < \infty,
\end{aligned} \tag{4}$$

where $Y(t) = (S_h, I_h, C_h, V_h, R_h, S_r, I_r, R_r)$ in Eq. (4) and contain variable X, which is;

$$X(t,Y(t)) = \begin{pmatrix} X_1(t,S_h(t)) \\ X_2(t,I_h(t)) \\ X_3(t,C_h(t)) \\ X_4(t,V_h(t)) \\ X_5(t,R_h(t)) \\ X_6(t,S_r(t)) \\ X_7(t,I_r(t)) \\ X_8(t,R_r(t)) \end{pmatrix}$$

$$= \begin{pmatrix} \Delta_1 - \left(\beta_1 \frac{I_h}{N_h} + \beta_2 \frac{I_r}{N_r} + \nu_h + \mu_h\right) S_h \\ \left(\beta_1' \frac{I_h(t-\tau_1)}{N_h(t-\tau_1)} + \beta_2' \frac{I_r(t-\tau_1)}{N_r(t-\tau_1)}\right) S_h(t-\tau_1) - (w_1 + \gamma + \nu_h + \vartheta_1) I_h \\ \gamma I_h - (\varsigma + \nu_h + \vartheta_2) C_h \\ \mu_h S_h - \nu_h V_h \\ \varsigma C_h + w_1 I_h - \nu_h R_h \\ \Delta_2 - \left(\frac{\beta_3 I_r}{N_r}\right) S_r - \nu_r S_r \\ \left(\frac{\beta_3' I_r(t-\tau_2)}{N_r(t-\tau_2)}\right) S_r(t-\tau_2) - (w_2 + \nu_r + \vartheta_3) I_r \\ w_2 I_r - \nu_r R_r \end{pmatrix}. \tag{5}$$

The concept from [41] and the Krasnoselkii fixed point theorem will now be used to demonstrate the existence of the solution for problem (4).

Theorem 1. *Let $(Z, \|.\|)$ is a Banach space, and B is closed and non empty subset of Banach space. Assume Λ_1 and Λ_2 are mappings from B to Z such that;*

- *for all $x, y \in B, \Lambda_1 x + \Lambda_2 y \in B$,*
- *Λ_1 is a contraction,*
- *Λ_2 is continuous and $\Lambda_2(B)$ is contained in a compact set.*

Then there exist $z \in B$ such that $z = \Lambda_1 z + \Lambda_2 z$
writing X as

$$X(t,Y(t),Y(t-\tau)) = X_1(t,Y(t),Y(t-\tau)) + X_2(t,Y(t),Y(t-\tau)),$$

wherein Lipschitz continuous are $X_i, i = 1,2$ and Lipschitz constants are $\mathcal{L}_i, i = 1,2$, respectively. Define $\Sigma = \Sigma_1 + \Sigma_2$ where

$$\Sigma_1 Y(t) = \varphi(0) + \frac{1}{\Gamma(\alpha)} \int_0^t X_1(\theta, Y(\theta)) (t-\theta)^{\alpha-1} d\theta,$$
$$\Sigma_2 Y(t) = \frac{1}{\Gamma(\alpha)} \int_0^t X_2(\theta, Y(\theta-\tau)) (t-\theta)^{\alpha-1} d\theta,$$

and let $W = [-\tau, \Im]$,

$$\|Y(t)\| = \sup_{t\in W} \|Y(t)\|.$$

To show Σ_1 *is contraction*

$$\begin{aligned}
\|\Sigma_1 Y_1(t) - \Sigma_1 Y_2(t)\| &\leq \frac{1}{\Gamma(\alpha)} \int_0^t \|\Sigma_1(\theta, Y_1(\theta)) - \Sigma_1(\theta, Y_2(\theta))\|(t-\theta)^{\alpha-1}\, d\theta, \\
&\leq \frac{\mathcal{L}_\infty}{\Gamma(\alpha)} \int_0^t \|Y_1(\theta) - Y_2(\theta)\|(t-\theta)^{\alpha-1}\, d\theta, \\
&\leq \frac{\mathcal{L}_\infty}{\Gamma(\alpha)} \|Y_1 - Y_2\| \int_0^t (t-\theta)^{\alpha-1}\, d\theta, \\
&\leq \frac{\mathcal{L}_\infty}{\Gamma(\alpha+1)} \|Y_1 - Y_2\| \Im^\alpha.
\end{aligned}$$

Thus Σ_1 *is contraction whenever* $\frac{\mathcal{L}_\infty \Im^\alpha}{\Gamma(\alpha+1)}\|Y_1 - Y_2\| \leq 1$.
Also, X_i*'s*

$$\begin{aligned}
\|X_1(t, Y(t))\| &\leq M_1 \|Y(t)\|, \\
\|X_2(t, Y(t-\tau))\| &\leq M_2 \|Y(t)\|.
\end{aligned}$$

Let $\mathcal{C}(W, \mathbb{R}^8)$ *denotes the set of bounded and continuous functions* W *to* $\mathbb{R}^8$ *and* B *described as;*

$$B = \{Y \in \mathcal{C} : \|Y\| \leq c\},$$

where c *satisfies*

$$\|\varphi(0)\| + \frac{(M_1 + M_2)c}{\Gamma(\alpha+1)} \Im^\alpha \leq c.$$

For $Y \in B$,

$$\begin{aligned}
\|\Sigma\| &= \|\Sigma_1 Y(t) + \Sigma_2 Y(t)\|, \\
&\leq \|\varphi(0)\| + \frac{1}{\Gamma(\alpha)} \int_0^t \|X_1(\theta, Y(\theta)) + X_2(\theta, Y(\theta-\tau))\|(t-\theta)^{\alpha-1} d\theta, \\
&\leq \|\varphi(0)\| + \frac{(M_1 + M_2)\|Y\|}{\Gamma(\alpha)} \int_0^t (t-\theta)^{\alpha-1} d\theta, \\
&\leq \|\varphi(0)\| + \frac{(M_1 + M_2)c}{\Gamma(\alpha+1)} \Im^\alpha.
\end{aligned}$$

Therefore $\Sigma_1 Y + \Sigma_2 Y \in B$. *Moreover, for* $Y \in B$, *we obtain*

$$\|\Sigma_2 Y(t)\| \leq \frac{1}{\Gamma(\alpha)} \int_0^t \|X_2(\theta, Y(\theta-\tau))\|(t-\theta)^{\alpha-1} d\theta,$$

$$\leq \frac{M_2\|Y\|}{\Gamma(\alpha)}\int_0^t (t-\theta)^{\alpha-1}d\theta \leq \frac{M_2 c}{\Gamma(\alpha+1)}\Im^{\alpha} \leq c.$$

To prove the Σ_2 continuity, let $Y_n \to Y$ be convergent sequence, such that;

$$\begin{aligned}\|\Sigma_2 Y_n(t) - \Sigma_2 Y(t)\| &\leq \frac{1}{\Gamma(\alpha)}\int_0^t \|X_2(\theta, Y_n(\theta-\tau)) - X_2(\theta, Y(\theta-\tau))\|(t-\theta)^{\alpha-1}d\theta,\\ &\leq \frac{\mathcal{L}_2}{\Gamma(\alpha)}\int_0^t \|Y_n(\theta-\tau) - Y(\theta-\tau)\|(t-\theta)^{\alpha-1}d\theta,\\ &\leq \frac{\mathcal{L}_2\|Y_n - Y\|}{\Gamma(\alpha)}\int_0^t (t-\theta)^{\alpha-1}d\theta \leq \frac{\mathcal{L}_2\|Y_n - Y\|}{\Gamma(\alpha+1)}\Im^{\alpha}.\end{aligned}$$

Therefore, $\Sigma_2 Y_n \to \Sigma_2 Y$, whenever $Y_n \to Y$. Continuity of Σ_2 established.

Next to show that $\Sigma_2(B)$ is subset of compact set, for any $t_1 \leq t_2 \leq \Im$,

$$\begin{aligned}\|\Sigma_2 Y(t_2) - \Sigma_2 Y(t_1)\| &\leq \frac{1}{\Gamma(\alpha)}\Big\| \int_0^{t_2} \Sigma_2(\theta, Y(\theta-\tau))(t_2-\theta)^{\alpha-1}d\theta\\ &\quad - \int_0^{t_1} \Sigma_2(\theta, Y(\theta-\tau))(t_1-\theta)^{\alpha-1}d\theta\Big\|,\\ &\leq \frac{1}{\Gamma(\alpha)}\int_0^{t_1} |(t_2-\theta)^{\alpha-1} - (t_1-\theta)^{\alpha-1}| * \|\Sigma_2(\theta, Y(\theta-\tau))\|d\theta\\ &\quad + \int_{t_1}^{t_2} |(t_2-\theta)^{\alpha-1}| * \|\Sigma_2(\theta, Y(\theta-\tau))\|d\theta,\\ &\leq \frac{M_2 c}{\Gamma(\alpha)}\int_0^{t_1} |(t_2-\theta)^{\alpha-1} - (t_1-\theta)^{\alpha-1}|d\theta + \frac{M_2 c}{\Gamma(\alpha)}\int_{t_1}^{t_2} |(t_2-\theta)^{\alpha-1}|d\theta,\\ &\leq \frac{M_2 c}{\Gamma(\alpha)}(t_2-t_1)^{\alpha}.\end{aligned}$$

Since a term above's right hand portion is free of y. As a result, $\Sigma_2(B)$ iS compact relatively, and Σ_2 is compact according to the Arzela-AScoli theorem. Consequently, all the conditions for applying Krasnoselskii's fixed point theorem met, As a result $Y \in B$, a fixed point of Σ, exist.

Theorem 2. *If the equation of the model* (4) *satisfied both conditions $\frac{\mathcal{L}_1\Im^{\alpha}}{\Gamma(\alpha+1)}\|Y_1 - Y_2\| < 1$ and $\|\varphi(0)\| + \frac{(M_1+M_2)c}{\Gamma(\alpha+1)}\Im^{\alpha} \leq c$, then model has unique solution in B.*

Let us now demonstrate the uniqueness of the system (4) solution.

Theorem 3. *Let $(0,\varphi) \in \Pi$, then the Eq.* (4) *has a unique solution through $(0,\varphi)$, where $X : \Pi \to \mathbb{R}^8$ is continuous, φ is an open set in $W \times \mathcal{C}$, and X is continuous as Lipschitz for every compact set in Π.*

Since all requirements for applying above theorems are met, there is only one solution to Eq. (4).

4.2. Non-negativity of the solution

Theorem 4. *The model* (3) *with* (2) *is positively invariant and bounded if*

$$\Omega = \begin{cases} (S_h, I_h, C_h, V_h, R_h) \subset \mathbb{R}^5_+ : S_h + E_h + I_h + C_h + V_h + R_h \leq \frac{\Delta_1}{\nu_h}, \\ (S_r, I_r, R_r) \subset \mathbb{R}^3_+ : S_r + I_r + R_r \leq \frac{\Delta_2}{\nu_r}. \end{cases}$$

Proof. Summation of first five equations of (3), we have

$$D_t^\alpha S_h + (\delta_h + \nu_h + \mu_h) S_h = \Delta_1. \tag{6}$$

The non-negativity of the RHS of (6) suggests

$$D_t^\alpha S_h + (\delta_h + \nu_h + \mu_h) S_h \geq 0. \tag{7}$$

Taking Laplace transformation of (7), we get

$$S_h(s) \geq \frac{s^{\alpha-1}}{(s^\alpha + (\delta_h + \nu_h + \mu_h))} S_h(0). \tag{8}$$

Applying inverse Laplace transformation we have

$$S_h(t) \geq E_{\alpha,1}(-(\delta_h + \nu_h + \mu_h) t^\alpha) S_h(0). \tag{9}$$

If $S_h(0)$ is positive, the right hand side of (9) will be positive. Hence we have $S_h(t) \geq 0$ for all $t \geq 0$. The corresponding non-negativity for other classes of (3) can be proven similarly.

We will proceeds now to prove that model (3) is bounded, for this, we sum first five equations of (3).

$$D_t^\alpha N_h(t) \leq \Delta_1 - \nu_h N_h(t), \tag{10}$$

and the additional three equations' summing yields;

$$D_t^\alpha N_r(t) \leq \Delta_2 - \nu_r N_h(r). \tag{11}$$

After the application of the Laplace transform to both Eqs. (10) and (11), the following outcomes were obtained;

$$N_h(t) \leq N_h(0) E_\alpha(-\nu_h t^\alpha) + \frac{\Delta_1}{\nu_h}(1 - E_\alpha(-\nu_h t^\alpha)), \tag{12}$$

$$N_r(t) \leq N_r(0) E_\alpha(-\nu_r t^\alpha) + \frac{\Delta_2}{\nu_r}(1 - E_\alpha(-\nu_r t^\alpha)). \tag{13}$$

As mittag leffler function (denoted by $E_{a,b}$) has asymptotic nature, which shows that as $t \to \infty$ gives $N_h(t) \leq \frac{\Delta_1}{\nu_h}$. We have $\sup N_h(t) \leq \frac{\Delta_1}{\nu_h}$. Also $N_h(t)$ is bounded if $N_h(0) \leq \frac{\Delta_1}{\nu_h}$, boundedness of $N_r(t)$ can be proven in similar approach.

4.3. Equilibrium points

For perceiving zero solution i.e. equilibrium points, of the model (3) setting right hand side equal to zero we get;

$$\begin{aligned}
&\Delta_1 - \delta_h S_h - (\nu_h + \mu_h)S_h = 0,\\
&\delta_h^{'} S_h(t-\tau_1) - (w_1 + \gamma + \nu_h + \vartheta_1)I_h = 0,\\
&\gamma I_h - (\varsigma + \nu_h + \vartheta_2)C_h = 0,\\
&\mu_h S_h - \nu_h V_h = 0,\\
&\varsigma C_h + w_1 I_h - \nu_h R_h = 0,\\
&\Delta_2 - \delta_r S_r - \nu_r S_r = 0,\\
&\delta_r^{'} S_r(t-\tau_2) - (w_2 + \nu_r + \vartheta_3)I_r = 0,\\
&w_2 I_r - \nu_r R_r = 0,
\end{aligned} \tag{14}$$

The disease-free equilibrium is known as the stage that occur when no disease in the population, which is portrayed in model as $I_h(0) = 0, C_h(0) = 0, I_r(0) = 0$.

The following is a point of disease free equilibrium:

$$\varpi^0(S_h^0, I_h^0, C_h^0, V_h^0, R_h^0, S_r^0, I_r^0, R_r^0) = \left(\frac{\Delta_1}{(\mu_h + \nu_h)}, 0, 0, \frac{\mu_h \Delta_1}{\nu_h(\mu_h + \nu_h)}, 0, \frac{\Delta_2}{\nu_r}, 0, 0\right). \tag{15}$$

In endemic equilibrium, disease cannot be totally removed from the population, so for calculating the endemic equilibrium point, all individual compartments must be nonzero. The point $\varpi^*(S_h^*, I_h^*, C_h^*, V_h^*, R_h^*, S_r^*, I_r^*, R_r^*)$ is driven by concurrently solving the Eq. (15), keeping in mind the requirement that every element of ϖ^* be non-zero.

4.4. Basic reproduction number

Regarding the time course of the epidemic, a key factor to take into account is the basic reproduction number giving the overall number of secondary infections produced by a single infective individual over its infectious period. The threshold R_0 was calculated according to the method of [42], [43]. Our estimation of the basic reproduction number of our model is more concentrated on the levels of prevalence among cases and infected human and rodent populations. In particular, the infectious compartments being investigated are referred to here as I_h, C_h and I_r. Take $\zeta = (I_h, C_h, I_r)$ where $(\cdot)^T$ denotes the transposition. Applying Diekmannetal's Ref. [42] next generation approach, the mathematical formulation of the infected population can be rewritten as:

$$\frac{d\zeta}{dt} = \mathcal{F}(\zeta) - \mathcal{V}(\zeta), \tag{6.6}$$

where

$$\mathcal{F} = \begin{pmatrix} \left(\beta_1' \frac{I_h(t-\tau_1)}{N_h(t-\tau_1)} + \beta_2' \frac{I_r(t-\tau_1)}{N_r(t-\tau_1)}\right) \\ 0 \\ \frac{\beta_3' S_r(t-\tau_2) I_r(t-\tau_2)}{N_r(t-\tau_2)} \end{pmatrix}, \quad \mathcal{V} = \begin{pmatrix} (w_1+\gamma+\nu_h+\vartheta_1)I_h \\ -\gamma I_h + (\varsigma+\nu_h+\vartheta_2)C_h \\ (w_2+\vartheta_3+\nu_r)I_r \end{pmatrix}. \tag{16}$$

Jacobian matrices for (32) at DFE (ϖ^0) is given by

$$\mathbf{F} = \begin{pmatrix} \frac{\beta_1' S_h^0}{N_h^0} & 0 & \frac{\beta_2' S_h^0}{N_r^0} \\ 0 & 0 & 0 \\ 0 & 0 & \frac{\beta_3' S_r^0}{N_r^0} \end{pmatrix}, \mathbf{V} = \begin{pmatrix} w_1+\gamma+\nu_h+\vartheta_1 & 0 & 0 \\ -\gamma & \varsigma+\nu_h+\vartheta_2 & 0 \\ 0 & 0 & w_2+\vartheta_3+\nu_r \end{pmatrix}. \tag{6.8}$$

So we get

$$\mathbf{F}\mathbf{V}^{-1} = \begin{pmatrix} \frac{\beta_1' S_h^0}{(w_1+\gamma+\nu_h+\vartheta_1)N_h^0} & 0 & \frac{\beta_2' S_h^0}{(w_2+\vartheta_3+\nu_r)N_r^0} \\ 0 & 0 & 0 \\ 0 & 0 & \frac{\beta_3' S_r^0}{(w_2+\vartheta_3+\nu_r)N_r^0} \end{pmatrix}. \tag{6.10}$$

The most prominent eigenvalue for the next-generation matrix $\mathbf{F}\mathbf{V}^{-1}$ is referred to as the basic reproduction number.

In this case, R_0 is provided by

$$R_0 = \max\{R_{h_0}, R_{r_0}\},$$

where R_{h_0} and R_{r_0} represent the reproduction number generated by humans and non-humans respectively, and using the values of ϖ^0 we get reproduction number as follow;

$$R_{h_0} = \frac{\beta_1' \nu_h}{(\nu_h+\mu_h)(w_1+\gamma+\nu_h+\vartheta_1)},$$
$$R_{r_0} = \frac{\beta_3'}{(w_2+\vartheta_3+\nu_r)}.$$

4.5. Sensitivity analysis

This subsection presents an analysis of the factors influencing the basic reproduction number R_0 within the specified model (3). A sensitivity analysis was conducted to evaluate the impact of various parameters, involving the calculation of the sensitivity index, which quantifies the significance of each parameter in relation to disease frequency and transmission. An analytical expression for the sensitivity index can be derived using the explicit formula for R_0.

$$si_{\delta}^{R_0} = \frac{\delta}{R_0}\left[\frac{\partial R_0}{\partial \delta}\right]. \tag{17}$$

Tables 2 and 3 display the derived sensitivity index depending on the corresponding parameters of R_{h_0} and R_{r_0}, while Figure 2a and 2b exhibit a graphical illustration of the data. The sensitivity index of a parameter can be used to determine how it affects the reproduction number. A positive index means that increasing the parameter will raise R_0, whereas a negative index means that increasing the parameter will decrease R_0. Only β_1 and β_3 have positive indices among these parameters, indicating that minimizing them will help manage the endemic. Furthermore, γ has the least effect on the sensitivity, whereas β_1 and β_3 have the most, suggesting that managing β_1 and β_3 is more successful than controlling γ. Additionally, our analysis provides that the vaccination index rate is -0.7356, meaning that more vaccinations prevent the disease from spreading. This mathematical insight illustrates the influence of vaccination on endemics.

Parameter	Sensitivity index	Value	Sign
w_1	$si_{w_1}^{R_0}$	-0.8383	-ve
β_1	$si_{\beta_1}^{R_0}$	1	+ve
ν_h	$si_{\nu_h}^{R_0}$	-0.0207	-ve
γ	$si_{\gamma}^{R_0}$	-0.0034	-ve
μ_h	$si_{\mu_h}^{R_0}$	-0.7356	-ve
ϑ_1	$si_{\vartheta_1}^{R_0}$	-0.00389	-ve

Table 2: Sensitive index of R_{h_0}

Parameter	Sensitivity index	Value	Sign
β_3	$si_{\beta_3}^{R_0}$	1	+ve
w_2	$si_{w_2}^{R_0}$	-0.3040	-ve
ϑ_3	$si_{\vartheta_3}^{R_0}$	-0.1465	-ve
ν_r	$si_{\nu_r}^{R_0}$	-0.54945	-ve

Table 3: Sensitive index of R_{r_0}

4.6. Stability analysis

4.6.1. Stability of disease free equilibrium

This subsection discusses the stability of disease-free equilibrium (DFE) in two scenarios: $\tau_1 = \tau_2 = 0$ and $\tau_1 > 0, \tau_2 > 0$.

Without Delay $(i.e. \tau_1 = \tau_2 = 0)$

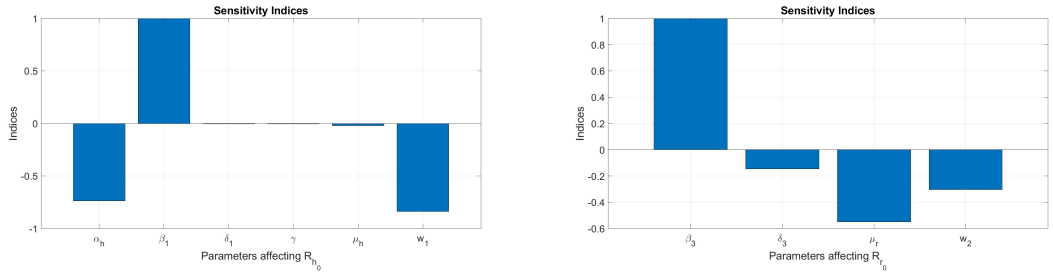

(a) (b)

Figure 2: Plot of sensitive indices of the parameters of R_0.

The following is the Jacobian matrix of system (3) at DFE without delay;

$$J = \begin{pmatrix} -\delta_h - (\nu_h + \mu_h) & \frac{-\beta_1 S_h(0)}{N_h(0)} & 0 & 0 & 0 & 0 & \frac{-\beta_2 S_h(0)}{N_r(0)} & 0 \\ \delta_h & \frac{\beta_1 S_h(0)}{N_h(0)} - (w_1 + \gamma + \nu_h + \vartheta_1) & 0 & 0 & 0 & 0 & \frac{\beta_2 S_h(0)}{N_r(0)} & 0 \\ 0 & \gamma & -(\varsigma + \nu_h + \vartheta_2) & 0 & 0 & 0 & 0 & 0 \\ \mu_h & 0 & 0 & -\nu_h & 0 & 0 & 0 & 0 \\ 0 & w_1 & \varsigma & 0 & -\nu_h & 0 & 0 & 0 \\ 0 & 0 & 0 & 0 & 0 & -\delta_r - \nu_r & \frac{-\beta_3 S_r(0)}{N_r(0)} & 0 \\ 0 & 0 & 0 & 0 & 0 & -\delta_r & \frac{\beta_3 S_r(0)}{N_r(0)} - (w_2 + \vartheta_3 + \nu_r) & 0 \\ 0 & 0 & 0 & 0 & 0 & 0 & w_2 & -\nu_r \end{pmatrix} \tag{18}$$

For simplicity, Let $k_1 = \nu_h + \mu_h, k_2 = w_1 + \gamma + \nu_h + \vartheta_1, k_3 = \varsigma + \nu_h + \vartheta_2, k_4 = w_2 + \vartheta_3 + \nu_r$ and using the Eq. (15) we get;

$$J = \begin{pmatrix} -k_1 & \frac{-\beta_1 \nu_h}{(\mu_h + \nu_h)} & 0 & 0 & 0 & 0 & -\beta_2 & 0 \\ 0 & \frac{\beta_1 \nu_h}{(\mu_h + \nu_h)} - k_2 & 0 & 0 & 0 & 0 & \beta_2 & 0 \\ 0 & \gamma & -k_3 & 0 & 0 & 0 & 0 & 0 \\ \mu_h & 0 & 0 & -\nu_h & 0 & 0 & 0 & 0 \\ 0 & w_1 & \varsigma & 0 & -\nu_h & 0 & 0 & 0 \\ 0 & 0 & 0 & 0 & 0 & -\nu_r & -\beta_3 & 0 \\ 0 & 0 & 0 & 0 & 0 & 0 & \beta_3 - k_4 & 0 \\ 0 & 0 & 0 & 0 & 0 & 0 & w_2 & -\nu_r \end{pmatrix}. \tag{19}$$

The characteristic polynomial of J is given by;

$$(\lambda + k_3)(\lambda + k_1)(\lambda + \nu_h)^2(\lambda + \nu_r)^2(\lambda + k_4 - \beta_3)\left(\lambda + k_2 - \frac{\beta_1 \nu_h}{(\mu_h + \nu_h)}\right). \tag{20}$$

It is quite straightforward to see that all zeros of Eq. (20) carry negative real values whenever $R_0 \leq 1$, which is in keeping with the Routh-Hurwitz criterion [44]. As a result, DFE is locally stable when $R_0 \leq 1$. Nevertheless, DFE becomes unstable if $R_0 \geq 1$, Eq. (20) has a positive solution.

With Delay(i.e. $\tau_1 > 0, \tau_2 > 0$**)**

The following is the Jacobian matrix of system (3) at DFE with delay;

$$det\begin{pmatrix} \tilde{a}_{11}-\lambda & \frac{-\beta_1 S_h(0)}{N_h(0)} & 0 & 0 & 0 & 0 & \frac{-\beta_2 S_h(0)}{N_r(0)} & 0 \\ \delta_h & \tilde{a}_{22}-\lambda & 0 & 0 & 0 & 0 & \frac{\beta_2' S_h(0)}{N_r(0)} e^{-\lambda\tau_1} & 0 \\ 0 & \gamma & \tilde{a}_{33}-\lambda & 0 & 0 & 0 & 0 & 0 \\ \mu_h & 0 & 0 & -\nu_h-\lambda & 0 & 0 & 0 & 0 \\ 0 & w_1 & \varsigma & 0 & -\nu_h-\lambda & 0 & 0 & 0 \\ 0 & 0 & 0 & 0 & 0 & -\delta_r-\nu_r-\lambda & \frac{-\beta_3 S_r(0)}{N_r(0)} & 0 \\ 0 & 0 & 0 & 0 & 0 & -\delta_r & \tilde{a}_{77}-\lambda & 0 \\ 0 & 0 & 0 & 0 & 0 & 0 & w_2 & -\nu_r-\lambda \end{pmatrix} = 0, \tag{21}$$

where $\tilde{a}_{11} = -\delta_h - (\nu_h + \mu_h), \tilde{a}_{22} = \frac{\beta_1' S_h(0)}{N_h(0)} e^{-\lambda\tau_1} - (w_1 + \gamma + \nu_h + \vartheta_1), \tilde{a}_{33} = -(\varsigma + \nu_h + \vartheta_2), \tilde{a}_{77} = \frac{\beta_3' S_r(0)}{N_r(0)} e^{-\lambda\tau_2} - (w_2 + \vartheta_3 + \nu_r)$.

Now, the characteristic equation of the matrix (21) is;

$$Y_0(\lambda) + Y_1(\lambda)e^{-\lambda\tau_1} + Y_2(\lambda)e^{-\lambda\tau_2} + Y_3(\lambda)e^{-\lambda(\tau_1+\tau_2)} = 0, \tag{22}$$

where

$$\begin{aligned} Y_0(\lambda) &= \lambda^8 + y_{01}\lambda^7 + y_{02}\lambda^6 + y_{03}\lambda^5 + y_{04}\lambda^4 + y_{05}\lambda^3 + y_{06}\lambda^2 + y_{07}\lambda + y_{08}, \\ Y_1(\lambda) &= y_{11}\lambda^7 + y_{12}\lambda^6 + y_{13}\lambda^5 + y_{14}\lambda^4 + y_{15}\lambda^3 + y_{16}\lambda^2 + y_{17}\lambda + y_{18}, \\ Y_2(\lambda) &= y_{21}\lambda^7 + y_{22}\lambda^6 + y_{23}\lambda^5 + y_{24}\lambda^4 + y_{25}\lambda^3 + y_{26}\lambda^2 + y_{27}\lambda + y_{28}, \\ Y_3(\lambda) &= y_{31}\lambda^6 + y_{32}\lambda^5 + y_{33}\lambda^4 + y_{34}\lambda^3 + y_{35}\lambda^2 + y_{36}\lambda + y_{37}. \end{aligned} \tag{23}$$

For an equation like (22), **(author?)** [45] provided a method for determining stability switching curves. Thus, by substituting $\lambda = i\lambda(\lambda > 0)$ in (22), using the same procedures. Identifying the set Ω, or each value of λ such that;

$$\left||Y_0|^2 + |Y_1|^2 - |Y_2|^2 - |Y_3|^2\right| \leq 2\sqrt{A_1^2 + B_1^2}, \tag{24}$$

in order to determine that $P(\lambda) = 0$ where,

$$\begin{aligned} P(\lambda) := \left(Y_0|^2 + |Y_1|^2 - |Y_2|^2 - |Y_3|^2\right)^2 - 4\left(A_1^2 + B_1^2\right), \\ A_1 := Re(Y_2\tilde{Y_3}) - Re(Y_0\tilde{Y_1}), \\ B_1 := Im(Y_2\tilde{Y_3}) - Im(Y_0\tilde{Y_1}). \end{aligned} \tag{25}$$

If there is a positive real solution to this equation, we can use the method described by [45] to discover the values of τ_1 and τ_2, switching curves. Thus, endemic equilibrium is stable under certain conditions. If not, we look into the circumstances in which this is completely stable.

Lemma 1. *Let*

$$\begin{aligned} Y_0(\mu) &= \mu^8 + y_{01}\mu^7 + y_{02}\mu^6 + y_{03}\mu^5 + y_{04}\mu^4 + y_{05}\mu^3 + y_{06}\mu^2 + y_{07}\mu + y_{08}, \\ Y_1(\mu) &= y_{11}\mu^7 + y_{12}\mu^6 + y_{13}\mu^5 + y_{14}\mu^4 + y_{15}\mu^3 + y_{16}\mu^2 + y_{17}\mu + y_{18}, \\ Y_2(\mu) &= y_{21}\mu^7 + y_{22}\mu^6 + y_{23}\mu^5 + y_{24}\mu^4 + y_{25}\mu^3 + y_{26}\mu^2 + y_{27}\mu + y_{28}, \\ Y_3(\mu) &= y_{31}\mu^6 + y_{32}\mu^5 + y_{33}\mu^4 + y_{34}\mu^3 + y_{35}\mu^2 + y_{36}\mu + y_{37}. \end{aligned} \tag{26}$$

where $\left|\frac{Y_{18}}{Y_{08}} + \frac{Y_{28}}{Y_{08}} + \frac{Y_{37}}{Y_{08}}\right| \leq 1$. *If* $M(\mu) = Y_0(\mu) + Y_1(\mu)e^{-\mu\tau_1} + Y_2(\mu)e^{-\mu\tau_2} + Y_3(\mu)e^{-\mu(\tau_1+\tau_2)}$ *and* $N(\mu) = Y_0(\mu)$, *where* $\tau_1, \tau_2 \geq 0$, *then* $M(\mu)$ *and* $N(\mu)$ *have an identical number of zeroes in their right half plane.*

Proof. Let

$$B_Q = \begin{cases} iQ(4t-1), & t \in \left[0, \frac{1}{2}\right], \\ Qexp\left(i\frac{\pi}{2}(3-4t)\right), & t \in \left(\frac{1}{2}, 1\right]. \end{cases} \tag{27}$$

Considering Q to be big enough, so that $|N(\mu)| > 0$, $\left|\frac{M(\mu)}{N(\mu)} - 1\right| \leq 1$ on B_Q. Therefore $|N(\mu) - M(\mu)| < |N(\mu)|$ on B_Q. Therefore, $M(\mu)$ and $N(\mu)$ are identical number of zeroes in B_Q, by Rouche's theorem.

Using Lemma 1 and the Routh-Hurwitz criterion, we arrive at the following conclusion.

Theorem 5. *If Routh-Hurwitz Criteria satisfied by* $Y_0(\lambda)$ *and* (22) *follows Lemma 1, then for any* $\tau_1, \tau_2 \geq 0$, *the roots of* (22) *possess a non-negative real component. Therefore, endemic equilibrium is stable absolutely for any delay.*

4.6.2. Stability of endemic equilibrium

Without Delay $(i.e. \tau_1 = \tau_2 = 0)$

The following is the Jacobian matrix of system (3) at endemic equilibrium without delay;

$$\begin{pmatrix} -\delta_h^* - (\nu_h + \mu_h) & \frac{-\beta_1 S_h^*}{N_h^*} & 0 & 0 & 0 & 0 & \frac{-\beta_2 S_h^*}{N_r^*} & 0 \\ \delta_h^* & \frac{\beta_1 S_h^*}{N_h^*} - (w_1 + \gamma + \nu_h + \vartheta_1) & 0 & 0 & 0 & 0 & \frac{\beta_2 S_h^*}{N_r^*} & 0 \\ 0 & \gamma & -(\varsigma + \nu_h + \vartheta_2) & 0 & 0 & 0 & 0 & 0 \\ \mu_h & 0 & 0 & -\nu_h & 0 & 0 & 0 & 0 \\ 0 & w_1 & \varsigma & 0 & -\nu_h & 0 & 0 & 0 \\ 0 & 0 & 0 & 0 & 0 & -\delta_r^* - \nu_r & \frac{-\beta_3 S_r^*}{N_r^*} & 0 \\ 0 & 0 & 0 & 0 & 0 & -\delta_r^* & \frac{\beta_3 S_r^*}{N_r^*} - (w_2 + \vartheta_3 + \nu_r) & 0 \\ 0 & 0 & 0 & 0 & 0 & 0 & w_2 & -\nu_r \end{pmatrix}. \tag{28}$$

The characteristic polynomial is given by;

$$\begin{aligned} & 2(\lambda+\nu_h)^2(\lambda+k_3)(\nu_r+\lambda) \\ & \left(-\frac{\lambda^2}{2}+\left(\frac{\beta_3 S_r^*}{2N_r^*}-\frac{\delta_r^*}{2}-\frac{k_4}{2}-\frac{\nu_r}{2}\right)\lambda\right. \\ & \left.+\left(\frac{\beta_3 S_r^*}{2N_r^*}-\frac{k_4}{2}\right)\nu_r+\delta_r^*\left(\beta_3 T_2-\frac{k_4}{2}\right)\right) \\ & \left(-\lambda^2+\left(\frac{S_h^*}{N_r^*}\beta_1-k_1-k_2+\delta_h\right)\lambda+\left(\frac{S_h^*}{N_r^*}\beta_1-k_2\right)k_1-\delta_h^* k_2\right), \end{aligned} \tag{29}$$

where $k_1=\nu_h+\mu_h, k_2=w_1+\gamma+\nu_h+\vartheta_1, k_3=\varsigma+\nu_h+\vartheta_2, k_4=w_2+\vartheta_3+\nu_r$.

It is quite straightforward to see that all zeros of Eq. (29) carry negative real values whenever $R_0\leq 1$, which is in keeping with the Routh-Hurwitz criterion [44]. As a result, DFE is locally stable when $R_0\leq 1$. Nevertheless, DFE becomes unstable if $R_0\geq 1$, Eq. (29) has a positive solution.

With Delay(i.e. $\tau_1>0,\tau_2>0$**)**

In order to talk about the stability of endemic equilibrium over time, we first linearize system (3) around $\breve{X}=(\breve{S}_h,\breve{I}_h,\breve{C}_h,\breve{V}_h,\breve{R}_h,\breve{S}_r,\breve{I}_r,\breve{R}_r)$ as any kind of equilibrium. Additionally, Let $S_h(t)=\breve{S}_h+x_1(t), I_h(t)=\breve{I}_h+x_2(t), C_h(t)=\breve{C}_h+x_3(t), V_h(t)=\breve{V}_h+x_4(t), R_h(t)=\breve{R}_h+x_5(t), S_r(t)=\breve{S}_r+x_6(t), I_r(t)=\breve{I}_r+x_7(t), R_r(t)=\breve{R}_r+x_8(t)$.

$$\breve{X}=PX(t)+QX(t-\tau_1)+RX(t-\tau_2), \tag{30}$$

where $X(t)=[x_1,x_2,x_3,x_4,x_5,x_6,x_7,x_8]^T$,

$$P=\begin{pmatrix} \breve{p}_{11} & \frac{-\beta_1\breve{S}_h}{\breve{N}_h} & 0 & 0 & 0 & 0 & \frac{-\beta_2\breve{S}_h}{\breve{N}_r} & 0 \\ 0 & \breve{p}_{22} & 0 & 0 & 0 & 0 & 0 & 0 \\ 0 & \gamma & \breve{p}_{33} & 0 & 0 & 0 & 0 & 0 \\ \mu_h & 0 & 0 & -\nu_h & 0 & 0 & 0 & 0 \\ 0 & w_1 & \varsigma & 0 & -\nu_h & 0 & 0 & 0 \\ 0 & 0 & 0 & 0 & 0 & \frac{-\beta_3\breve{I}_r}{\breve{N}_r}-\nu_r & \frac{-\beta_3\breve{S}_r}{\breve{N}_r} & 0 \\ 0 & 0 & 0 & 0 & 0 & 0 & \breve{p}_{77} & 0 \\ 0 & 0 & 0 & 0 & 0 & 0 & w_2 & -\nu_r \end{pmatrix}, \tag{31}$$

$$Q=\begin{pmatrix} 0 & 0 & 0 & 0 & 0 & 0 & 0 & 0 \\ \breve{q}_{21} & \breve{q}_{22} & 0 & 0 & 0 & 0 & \breve{q}_{27} & 0 \\ 0 & 0 & 0 & 0 & 0 & 0 & 0 & 0 \\ 0 & 0 & 0 & 0 & 0 & 0 & 0 & 0 \\ 0 & 0 & 0 & 0 & 0 & 0 & 0 & 0 \\ 0 & 0 & 0 & 0 & 0 & 0 & 0 & 0 \\ 0 & 0 & 0 & 0 & 0 & 0 & 0 & 0 \\ 0 & 0 & 0 & 0 & 0 & 0 & 0 & 0 \end{pmatrix}, \quad R=\begin{pmatrix} 0 & 0 & 0 & 0 & 0 & 0 & 0 & 0 \\ 0 & 0 & 0 & 0 & 0 & 0 & 0 & 0 \\ 0 & 0 & 0 & 0 & 0 & 0 & 0 & 0 \\ 0 & 0 & 0 & 0 & 0 & 0 & 0 & 0 \\ 0 & 0 & 0 & 0 & 0 & 0 & 0 & 0 \\ 0 & 0 & 0 & 0 & 0 & 0 & 0 & 0 \\ 0 & 0 & 0 & 0 & 0 & \breve{r}_{76} & \breve{r}_{77} & 0 \\ 0 & 0 & 0 & 0 & 0 & 0 & 0 & 0 \end{pmatrix}, \tag{32}$$

where $\breve{p}_{11} = \beta_1 \frac{\breve{I}_h}{\breve{N}_h} + \beta_2 \frac{\breve{I}_r}{\breve{N}_r} - (\nu_h + \mu_h), \breve{p}_{22} = -(w_1 + \gamma + \nu_h + \vartheta_1), \breve{p}_{33} = -(\varsigma + \nu_h + \vartheta_2), \breve{p}_{77} = -(w_2 + \vartheta_3 + \nu_r), \breve{q}_{21} = \beta_1' \frac{\breve{I}_h}{\breve{N}_h} + \beta_2' \frac{\breve{I}_r}{\breve{N}_r}, \breve{q}_{22} = \frac{\beta_1' \breve{S}_h}{\breve{N}_h}, \breve{q}_{27} = \frac{\beta_2' \breve{S}_h}{\breve{N}_r}, \breve{r}_{76} = \frac{\beta_3' \breve{I}_r}{\breve{N}_r}, \breve{r}_{77} = \frac{\beta_3' \breve{S}_r}{\breve{N}_r}.$

The characteristic equation of the system (30) is;

$$det \begin{pmatrix} \breve{p}_{11} - \lambda & \frac{-\beta_1 \breve{S}_h}{\breve{N}_h} & 0 & 0 & 0 & 0 & \frac{-\beta_2 \breve{S}_h}{\breve{N}_r} & 0 \\ (\breve{q}_{21})\, e^{-\lambda\tau_1} & (\breve{q}_{22})\, e^{-\lambda\tau_1} + \breve{p}_{22} - \lambda & 0 & 0 & 0 & 0 & \breve{q}_{27} e^{-\lambda\tau_1} & 0 \\ 0 & \gamma & \breve{p}_{33} - \lambda & 0 & 0 & 0 & 0 & 0 \\ \mu_h & 0 & 0 & -\nu_h - \lambda & 0 & 0 & 0 & 0 \\ 0 & w_1 & \varsigma & 0 & -\nu_h - \lambda & 0 & 0 & 0 \\ 0 & 0 & 0 & 0 & 0 & \frac{-\beta_3 \breve{I}_r}{\breve{N}_r} - \nu_r - \lambda & \frac{-\beta_3 \breve{S}_r}{\breve{N}_r} & 0 \\ 0 & 0 & 0 & 0 & 0 & \breve{r}_{76} e^{-\lambda\tau_2} & (\breve{r}_{77})\, e^{-\lambda\tau_2} - (w_2 + \vartheta_3 + \nu_r) - \lambda & 0 \\ 0 & 0 & 0 & 0 & 0 & 0 & w_2 & -\nu_r - \lambda \end{pmatrix} = 0. \tag{33}$$

The result is a transcendental polynomial that is provided by;

$$Y_0(\lambda) + Y_1(\lambda) e^{-\lambda\tau_1} + Y_2(\lambda) e^{-\lambda\tau_2} + Y_3(\lambda) e^{-\lambda(\tau_1+\tau_2)} = 0, \tag{34}$$

where

$$\begin{aligned} Y_0(\lambda) &= \lambda^8 + y_{01}\lambda^7 + y_{02}\lambda^6 + y_{03}\lambda^5 + y_{04}\lambda^4 + y_{05}\lambda^3 + y_{06}\lambda^2 + y_{07}\lambda + y_{08}, \\ Y_1(\lambda) &= y_{11}\lambda^7 + y_{12}\lambda^6 + y_{13}\lambda^5 + y_{14}\lambda^4 + y_{15}\lambda^3 + y_{16}\lambda^2 + y_{17}\lambda + y_{18}, \\ Y_2(\lambda) &= y_{21}\lambda^7 + y_{22}\lambda^6 + y_{23}\lambda^5 + y_{24}\lambda^4 + y_{25}\lambda^3 + y_{26}\lambda^2 + y_{27}\lambda + y_{28}, \\ Y_3(\lambda) &= y_{31}\lambda^6 + y_{32}\lambda^5 + y_{33}\lambda^4 + y_{34}\lambda^3 + y_{35}\lambda^2 + y_{36}\lambda + y_{37}. \end{aligned} \tag{35}$$

By using the same, above Theorem 5 and Lemma 1 we get the endemic stability of (3).

5. Numerical simulation and graph

5.1. Numerical scheme

To build an appropriate methodology for (3), we utilize predictor corrector method using Caputo derivative. The following is the editing system of (3);

$$\begin{cases} D_t^\alpha[S_h(t)] = \mathcal{X}_1(t, S_h(t)), \\ D_t^\alpha[E_h(t)] = \mathcal{X}_2(t, E_h(t)), \\ D_t^\alpha[I_h(t)] = \mathcal{X}_3(t, I_h(t)), \\ D_t^\alpha[C_h(t)] = \mathcal{X}_4(t, C_h(t)), \\ D_t^\alpha[V_h(t)] = \mathcal{X}_5(t, V_h(t)), \\ D_t^\alpha[R_h(t)] = \mathcal{X}_6(t, R_h(t)), \\ D_t^\alpha[S_r(t)] = \mathcal{X}_7(t, S_r(t)), \\ D_t^\alpha[I_r(t)] = \mathcal{X}_8(t, I_r(t)), \\ D_t^\alpha[R_r(t)] = \mathcal{X}_9(t, R_r(t)), \end{cases} \tag{36}$$

where

$$\begin{cases} \mathcal{X}_1(t,S_h(t)) = \Delta_1 - \left(\beta_1 \frac{I_h}{N_h} + \beta_2 \frac{I_r}{N_r}\right) S_h - (\nu_h + \mu_h) S_h, \\ \mathcal{X}_2(t,E_h(t)) = \left(\beta_1 \frac{I_h}{N_h} + \beta_2 \frac{I_r}{N_r}\right) S_h - \left(\beta_1' \frac{I_h(t-\tau_1)}{N_h(t-\tau_1)} + \beta_2' \frac{I_r(t-\tau_1)}{N_r(t-\tau_1)}\right) S_h(t-\tau_1) - \nu_h E_h, \\ \mathcal{X}_3(t,I_h(t)) = \left(\beta_1' \frac{I_h(t-\tau_1)}{N_h(t-\tau_1)} + \beta_2' \frac{I_r(t-\tau_1)}{N_r(t-\tau_1)}\right) S_h(t-\tau_1) - (w_1 + \gamma + \nu_h + \vartheta_1) I_h, \\ \mathcal{X}_4(t,C_h(t)) = \gamma I_h - (\varsigma + \nu_h + \vartheta_2) C_h, \\ \mathcal{X}_5(t,V_h(t)) = \mu_h S_h - \nu_h V_h, \\ \mathcal{X}_6(t,R_h(t)) = \varsigma C_h + w_1 I_h - \nu_h R_h, \\ \mathcal{X}_7(t,S_r(t)) = \Delta_2 - \left(\frac{\beta_3 I_r}{N_r}\right) S_r - \nu_r S_r, \\ \mathcal{X}_8(t,I_r(t)) = \left(\frac{\beta_3' I_r(t-\tau_2)}{N_r(t-\tau_2)}\right) S_r(t-\tau_2) - (w_2 + \nu_r + \vartheta_3) I_r, \\ \mathcal{X}_9(t,R_r(t)) = w_2 I_r - \nu_r R_r. \end{cases} \tag{37}$$

Hence, we can write model (3) as;

$$\begin{cases} D_t^{\alpha}[\Phi(t)] = \mathcal{X}(t,\Phi(t),\Phi(t-\tau)), \\ \Phi(t)(0) = f(t), \quad t \in [-\tau, 0]. \end{cases} \tag{38}$$

Now, utilizing the predictor corrector technique, we get;

$$\begin{aligned} \Phi(t) =& f(0) + \frac{h^{\alpha}}{\Gamma(\alpha+2)} \mathcal{X}(t_{m+1}, \Phi^p(t_{m+1}), \Phi^p(t_{m+1}-\tau)) \\ &+ \frac{h^{\alpha}}{\Gamma(\alpha+2)} \sum_{l=0}^{m} \delta_{l,m+1} \mathcal{X}(t_l, \Phi(t_l), \Phi(t_l-\tau)), \end{aligned} \tag{39}$$

where

$$\delta_{l,m+1} = \begin{cases} m^{\alpha+1} - (m-\alpha)(m+1)^{\alpha}, & l = 0, \\ (m-l+2)^{\alpha+1} + (m-l)^{\alpha+1} - 2(m-l+1)^{\alpha+1}, & 1 \le l \le m, \\ 1, & l = m+1, \end{cases} \tag{40}$$

and

$$\begin{aligned} \Phi^p(t_{m+1}) &= f(0) + \frac{1}{\Gamma(\alpha)} \sum_{l=0}^{m} \psi_{l,m+1} \mathcal{X}(t_l, \Phi(t_l), \Phi(t_l-\tau)), \\ \psi_{l,m+1} &= \frac{h^{\alpha}}{\alpha}((m+1-l)^{\alpha} - (m-l)^{\alpha}). \end{aligned} \tag{41}$$

5.2. Results and discussion

In this section, we provide a comprehensive analysis of the graphical outcomes associated with the proposed model (3). Due to the scarcity of empirical data on rodent populations and their epidemiological statistics specific to monkeypox, the initial values and parameters related to the rodent compartment were estimated by adapting transmission rates and population sizes from literature on zoonotic diseases. This approach ensures

Initial Condition	Value	Initial Condition	Value
$S_h(0)$	7900000000	$S_r(0)$	500
$E_h(0)$	10000000	$I_r(0)$	125
$I_h(0)$	4500	$R_r(0)$	50
$C_h(0)$	1000		
$V_h(0)$	1000000		
$R_h(0)$	3000		

Table 4: Initial condition of model (3) used in simulations

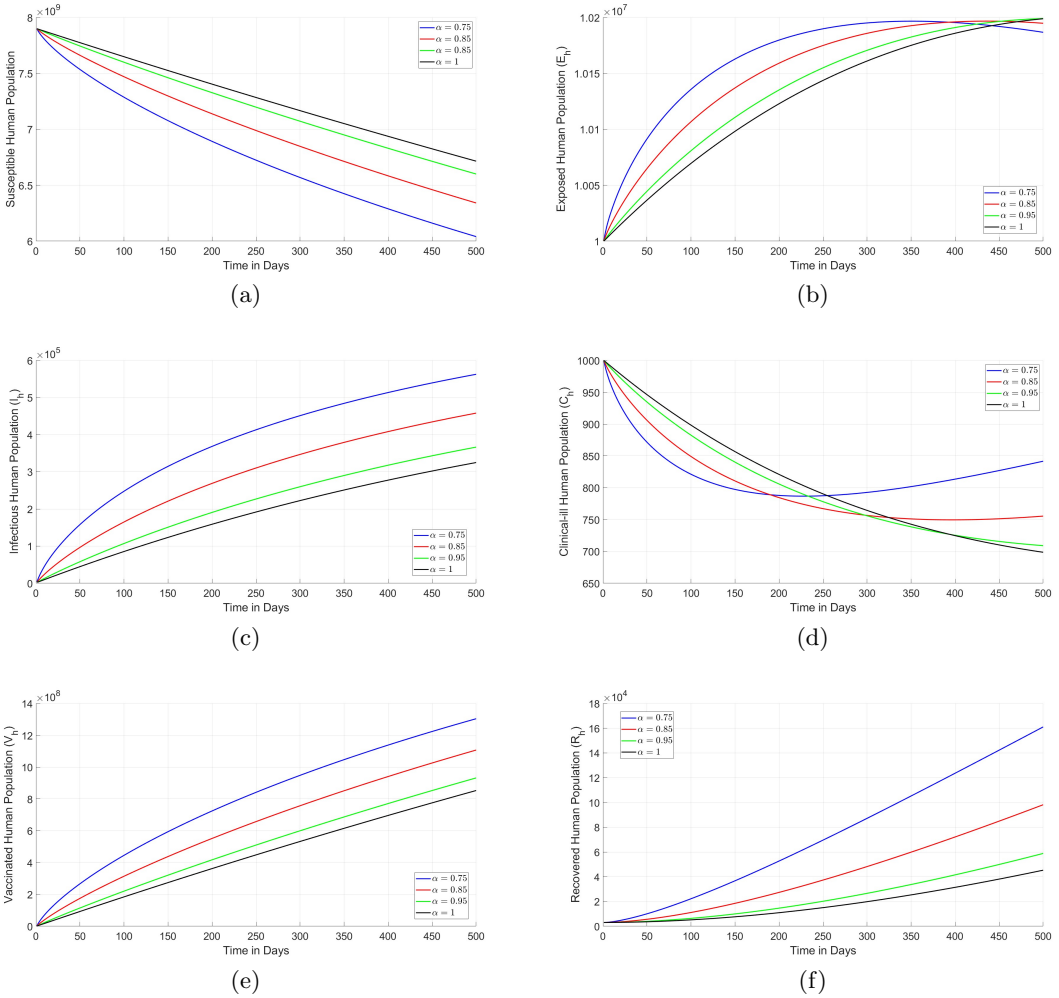

Figure 3: Simulation of human population dynamics with delays $\tau_1 = 7$ and $\tau_2 = 5$, using parameter value from Table 1, for fractional order $\alpha = 0.75, 0.85, 0.95, 1$.

the model's parameters are grounded in established epidemiological patterns, enhancing its applicability to real-world monkeypox dynamics. The complete set of initial condi-

tions and parameter values employed in the simulations are presented in Tables 4 and 1, respectively. Numerical experiments were implemented using MATLAB [46], a widely utilized platform for scientific computation. The numerical approximations were obtained by applying the discretization schemes defined in Eqs. (39) and (41), thereby ensuring both reliability and stability in the evaluation of the fractional-order delay model. These results yield significant insights into the transmission dynamics of monkeypox under the influence of delays and memory effects.

The graphical outcomes depicted in Figures 3–4 highlight the impact of the fractional derivative order α on the delayed dynamics of monkeypox spread. Here, $\tau_1 = 7$ days represents the average diagnosis delay in humans, while $\tau_2 = 5$ days denotes the corresponding diagnosis delay in rodents. The parameter α reflects the memory effects intrinsic to fractional-order models, where smaller values capture stronger non-local effects and slower system responses compared to the classical case $\alpha = 1$. The simulations demonstrate that the exposed human population (E_h) stabilizes over time, whereas the infected population (I_h) increases, indicating a clinical burden on healthcare systems, as represented by the growth in the clinically ill class (C_h). Simultaneously, a marked rise in the vaccinated population (V_h), coupled with a decline in both susceptible (S_h) and clinically ill individuals (C_h), underscores the role of vaccination as an effective intervention strategy. These findings align with real-world epidemiological observations, where timely vaccination campaigns can significantly reduce disease severity and incidence.

In Figure 5, we illustrate the impact of extending the delay parameters from $\tau_1 = 7$, $\tau_2 = 5$ days to $\tau_1 = 14$, $\tau_2 = 21$ days on the transmission dynamics of monkeypox. This adjustment significantly delays the predicted outbreak timelines. With shorter delays, the model forecasts outbreak scenarios within approximately 500 days. In contrast, longer delays extend predictions to over 1000 days, highlighting a substantial deviation from real-world disease progression. These extended delays present critical challenges for public health interventions, as delayed predictions may misguide disease control strategies, leading to prolonged outbreaks, increased transmission, and difficulties in implementing timely and effective mitigation measures in practical settings.

In Figure 6, we examine the effect of varying the human vaccination rate μ_h on the transmission dynamics of monkeypox, specifically focusing on the exposed (E_h), infected (I_h), and clinically ill (C_h) populations. As the vaccination rate μ_h increases from 0.25 to 0.85, a clear decline is observed across all three population classes. This reduction highlights the effectiveness of vaccination in mitigating disease spread, lowering the number of exposed and actively infected individuals, and ultimately reducing the clinical burden of monkeypox.

6. Conclusion

This study investigates the transmission of monkeypox disease in both human and rodent populations through the application of fractional order delay differential equations utilizing the Caputo derivative. The model encompasses the transmission dynamics of monkeypox in humans, represented by six compartments ($S_h(t), E_h(t), I_h(t), V_h(t), C_h(t),$

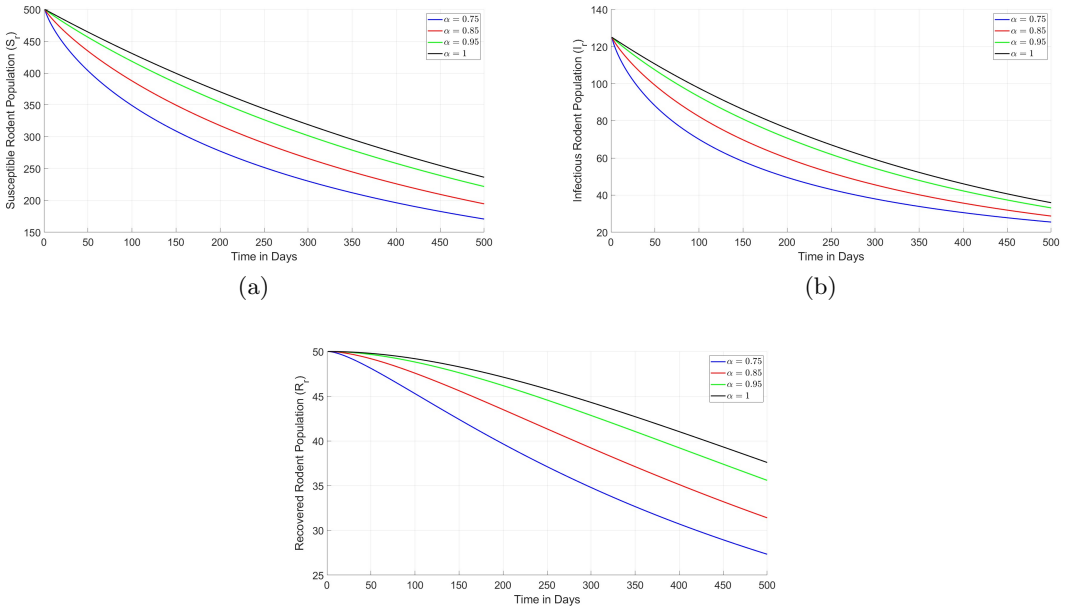

Figure 4: Simulation of rodent population dynamics with delays $\tau_1 = 7$ and $\tau_2 = 5$, using parameter value from Table (1), for fractional order $\alpha = 0.75, 0.85, 0.95, 1$.

$R_h(t)$), as well as three compartments associated with rodents $(S_r(t), I_r(t), R_r(t))$. Furthermore, the study explores the implications of vaccination and relevant clinical scenarios.

In the qualitative analysis, the existence and uniqueness of solutions are affirmed, alongside the positivity and boundedness of these solutions. The basic reproduction number is calculated employing next-generation matrix techniques, with normalized sensitivity indices for critical parameters of the basic reproduction number also determined. The stability of the model is established through the curve switching method, Routh-Hurwitz criteria, and Rouche's theorem. The theoretical findings are validated by numerical simulations and graphical representations, which illustrate the impact of delays within the infected and clinically ill populations, highlighting the significant role of vaccination in stabilizing disease dynamics and facilitating disease eradication.

This research primarily focuses on the transmission dynamics of single diseases; however, the framework can be adapted to include scenarios involving co-infections, such as dengue, malaria, and HIV. Additionally, it can be enhanced through the incorporation of stochastic effects and alternative fractional operators, including ABC fractional derivative and generalized Caputo derivatives. Future studies assessing the cost-effectiveness of intervention strategies serve to provide a more comprehensive basis for improving epidemic management and guiding public health policy.

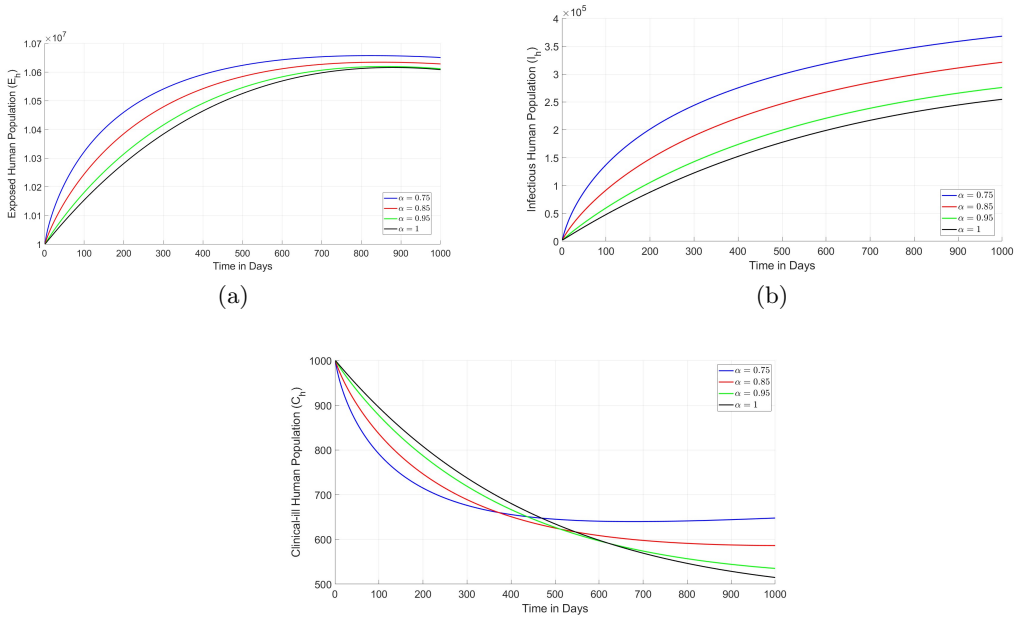

Figure 5: Simulation of E_h, I_h, and C_h population under different values of fractional order $\alpha = 0.75, 0.85, 0.95, 1$, using parameters value from Table (1), with delays $\tau_1 = 14$ and $\tau_2 = 21$.

Acknowledgements

Jatin Bansal, the author, expresses sincere gratitude to the University Grant Commission (UGC) for the generous financial support received in the form of a Senior Research Fellowship (JRF) as acknowledged in the UGC ID: 191620046310.
A.K, K.N and T.A would like to thank Prince Sultan University for the support through APC TAS research lab.

References

[1] WHO. WHO recommends new name for monkeypox disease. https://news.un.org/en/story/2022/11/1131082, 2022. Accessed: November 28, 2022.

[2] WHO. WHO Director-General declares mpox outbreak a public health emergency of international concern. WHO website, 2024. Accessed: August 14, 2024.

[3] Preben von Magnus, Else Krag Andersen, Knud Birkum Petersen, and Aksel Birch-Andersen. A pox-like disease in cynomolgus monkeys. *Acta Pathologica et Microbiologica Scandinavica*, 46(2):156–176, 1959.

[4] Isao Arita and Donald A. Henderson. Smallpox and monkeypox in non-human primates. *Bulletin of the World Health Organization*, 39(2):277–283, 1968.

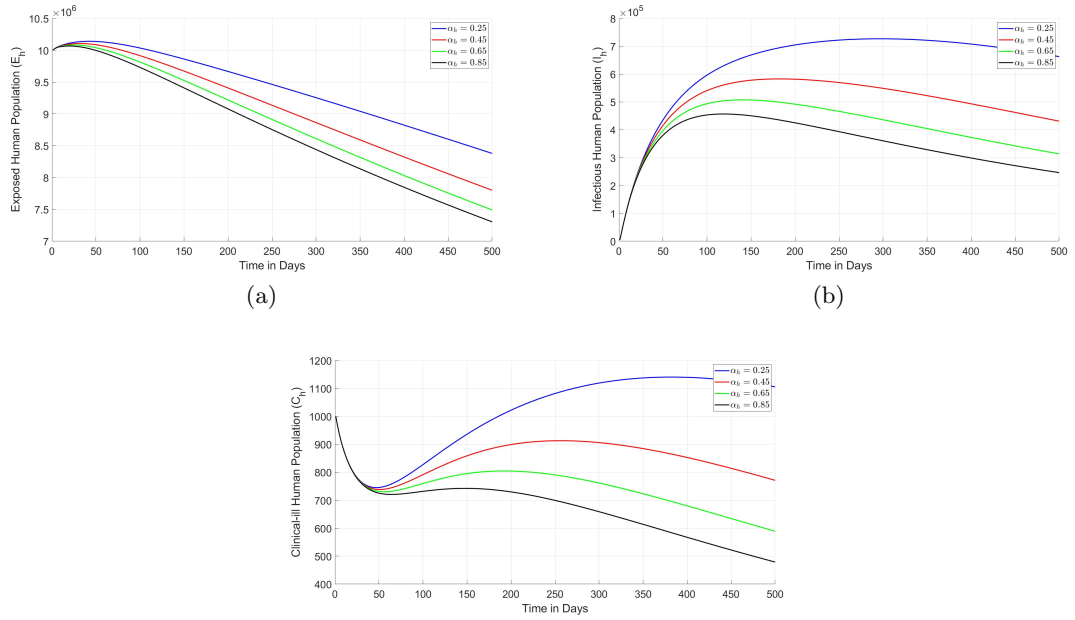

Figure 6: Simulation of E_h, I_h, and C_h population under different values of vaccination rate μ_h and other parameters value from Table (1), for fractional order $\alpha = 0.75, 0.85, 0.95, 1$ with delays $\tau_1 = 7$ and $\tau_2 = 5$.

[5] Stewart J. McConnell, Yaye F. Herman, Donald E. Mattson, and Leroy Erickson. Monkey pox disease in irradiated cynomolgus monkeys. *Nature*, 195(4846):1128–1129, 1962.

[6] J. C. Peters. A monkey-pox enzooty in the "Blijdorp" zoo. *Tijdschrift voor Diergeneeskunde*, 91(15):951–960, 1966.

[7] Joel G. Breman, Ruti Kalisa, M. V. Steniowski, E. Zanotto, A. I. Gromyko, and Isao Arita. Human monkeypox, 1970–79. *Bulletin of the World Health Organization*, 58(2):165–182, 1980.

[8] Isao Arita, Zdenek Jezek, Lev Khodakevich, and Kalisa Ruti. Human monkeypox: A newly emerged orthopoxvirus zoonosis in the tropical rain forests of africa. *The American Journal of Tropical Medicine and Hygiene*, 34(4):781–789, 1985.

[9] Paul E. M. Fine, Zdenek Jezek, Bernard Grab, and H. Dixon. The transmission potential of monkeypox virus in human populations. *International Journal of Epidemiology*, 17(3):643–650, 1988.

[10] WHO. Monkeypox Q and A: What you need to know about monkeypox. WHO website, 2022. Accessed: June 10, 2022.

[11] Fok-Moon Lum, Anthony Torres-Ruesta, Matthew Z. Tay, Raymond T. P. Lin, David C. Lye, Laurent Rénia, and Lisa F. P. Ng. Monkeypox: Disease epidemiology, host immunity and clinical interventions. *Nature Reviews Immunology*, 22(10):597–613, 2022.

[12] WHO. Clinical management and infection prevention and control for monkeypox: Interim rapid response guidance. Technical report, World Health Organization, Geneva, Switzerland, 2022. Accessed: 2022-06-10.

[13] WHO. Multi-country outbreak of mpox: External situation report 35. Technical report, World Health Organization, Geneva, Switzerland, 2024. Accessed: 2024-08-12.

[14] WHO. 2022-24 Mpox (Monkeypox) outbreak: Global trends. https://worldhealthorg.shinyapps.io/mpx$_global$/.

[15] U.S. Food and Drug Administration. Monkeypox (mpox) and Medical Devices. https://www.fda.gov/medical-devices/emergency-situations-medical-devices/monkeypox-mpox-and-medical-devicesCleared, 2024.

[16] WHO. Policy brief on vaccination against monkeypox in the who european region. Technical report, World Health Organization, Geneva, Switzerland, 2022. Accessed: 2022-08-26.

[17] Olumuyiwa James Peter, Afeez Abidemi, Mayowa M. Ojo, and Tawakalt Abosede Ayoola. Mathematical model and analysis of monkeypox with control strategies. *The European Physical Journal Plus*, 138(3):242, 2023.

[18] Jatin Bansal, Mehar Chand, Praveen Agarwal, Mansoor Alshehri, and Shilpi Jain. Extension of the truncated m-fractional derivative linked to multivariate generalized mittag-leffler function demonstrating classical characteristics. In *Fractional Differential Equations*, pages 1–10. Elsevier, 2024.

[19] Pushpendra Kumar, Madasamy Vellappandi, Zareen A. Khan, S. M. Sivalingam, Anthony Kaziboni, and Venkatesh Govindaraj. A case study of monkeypox disease in the united states using mathematical modeling. *Mathematics and Computers in Simulation*, 213:444–465, 2023.

[20] Rajermani Thinakaran, Somasekar Jalari, Vikram Neerugatti, Ravindra Raman Cholla, and K Nagendra Rao. Smart energy management system using iot for real-time monitoring and theft detection. In *2024 9th International Conference on Information Technology and Digital Applications (ICITDA)*, pages 1–5. IEEE, 2024.

[21] Jatin Bansal, Amit Kumar, Anoop Kumar, Aziz Khan, and Thabet Abdeljawad. Investigation of monkeypox disease transmission with vaccination effects using fractional order mathematical model under atangana-baleanu caputo derivative. *Modeling Earth Systems and Environment*, 11(1):1–40, 2025.

[22] Jaskirat Pal Singh, Sachin Kumar, Dumitru Baleanu, and Kottakkaran Sooppy Nisar. Monkeypox viral transmission dynamics and fractional-order modeling with vaccination intervention. *Fractals*, 31(8):2340096, 2023.

[23] Botao Liu, Samreen Farid, Saif Ullah, Mohamed Altanji, Rashid Nawaz, and Shewafera Wondimagegnhu Teklu. Mathematical assessment of monkeypox disease with the impact of vaccination using a fractional epidemiological modeling approach. *Scientific Reports*, 13(1):13550, 2023.

[24] Muhammad Bilal, Jingli Ren, and Usman Younas. Stability analysis and optical soliton solutions to the nonlinear schrödinger model with efficient computational techniques. *Optical and Quantum Electronics*, 53(7):406, 2021.

[25] Olumuyiwa James Peter, Sumit Kumar, Nitu Kumari, Festus Abiodun Oguntolu, Kayode Oshinubi, and Rabiu Musa. Transmission dynamics of monkeypox virus: A mathematical modelling approach. *Modeling Earth Systems and Environment*, 8(3):3423–3434, 2022.

[26] Marina Banuet-Martinez, Yang Yang, Behnaz Jafari, Avneet Kaur, Zahid A. Butt, Helen H. Chen, Svetlana Yanushkevich, Iain R. Moyles, Jane M. Heffernan, and Chapin S. Korosec. Monkeypox: A review of epidemiological modelling studies and how modelling has led to mechanistic insight. *Epidemiology and Infection*, 151:e121, 2023.

[27] Muhammad Younis, Muhammad Bilal, Shafqat ur Rehman, Usman Younas, and Syed Tahir Raza Rizvi. Investigation of optical solitons in birefringent polarization preserving fibers with four-wave mixing effect. *International Journal of Modern Physics B*, 34(11):2050113, 2020.

[28] Hasib Khan, Jehad Alzabut, DK Almutairi, Wafa Khalaf Alqurashi, Sandra Pinelas, Osman Tunã, and Mohammad Athar Azim. A coupled nonlinear system of integro-differential equations using modified abc operator. *FRACTALS (fractals)*, 33(06):1–14, 2025.

[29] Usman Younas, TA Sulaiman, and Jingli Ren. Diversity of optical soliton structures in the spinor bose–einstein condensate modeled by three-component gross–pitaevskii system. *International Journal of Modern Physics B*, 37(01):2350004, 2023.

[30] Suvankar Majee, Soovoojeet Jana, and T. K. Kar. Dynamical analysis of monkeypox transmission incorporating optimal vaccination and treatment with cost-effectiveness. *Chaos: An Interdisciplinary Journal of Nonlinear Science*, 33(4):043103, 2023.

[31] Waleed Adel, Amr Elsonbaty, Abdullah Aldurayhim, and Ahmed El-Mesady. Investigating the dynamics of a novel fractional-order monkeypox epidemic model with optimal control. *Alexandria Engineering Journal*, 73:519–542, 2023.

[32] Hasib Khan, Jehad Alzabut, DK Almutairi, Haseena Gulzar, and Wafa Khalaf Alqurashi. Data analysis of fractal-fractional co-infection covid-tb model with the use of artificial intelligence. *FRACTALS (fractals)*, 33(04):1–21, 2025.

[33] Misbah Ullah, Muhammad Sarwar, Hasib Khan, Thabet Abdeljawad, and Aziz Khan. Near-coincidence point results in metric interval space and hyperspace via simulation functions. *Advances in Difference Equations*, 2020(1):291, 2020.

[34] Rabab Alharbi, Rashid Jan, Sultan Alyobi, Yousif Altayeb, and Ziad Khan. Mathematical modeling and stability analysis of the dynamics of monkeypox via fractional-calculus. *Fractals*, 30(10):2240266, 2022.

[35] Changtong Li, Samreen, Saif Ullah, Rashid Nawaz, Salman A Alqahtani, and Shuo Li. Mathematical modeling and analysis of monkeypox 2022 outbreak with the environment effects using a cpauto fractional derivative. *Physica Scripta*, 98(10):105239, 2023.

[36] Philip N A. Akuka, Baba Seidu, and Mehmet Gümüş. Fractional-order modeling of monkeypox dynamics: Insights from optimal control. *Journal of Mathematics*, 2025(1):3060458, 2025.

[37] Igor Podlubny. *Fractional Differential Equations: An Introduction to Fractional*

Derivatives, Fractional Differential Equations, to Methods of Their Solution and Some of Their Applications, volume 198 of *Mathematics in Science and Engineering*. Academic Press, San Diego, CA, USA, 1998.

[38] Anatolii A. Kilbas, Hari M. Srivastava, and Juan J. Trujillo. *Theory and Applications of Fractional Differential Equations*, volume 204 of *North-Holland Mathematics Studies*. Elsevier Science, Amsterdam, Netherlands, 2006.

[39] United Nations Population Fund. World Population Dashboard. https://www.unfpa.org/data/world-population/WORLD, 2024.

[40] Christinah P. Bhunu and Steady Mushayabasa. Modelling the transmission dynamics of pox-like infections. *IAENG International Journal of Applied Mathematics*, 41(4):319–326, 2011.

[41] Syed Abbas. Existence of solutions to fractional order ordinary and delay differential equations and applications. *Electronic Journal of Differential Equations*, 2011(9):1–11, 2011.

[42] Odo Diekmann, J. A. P. Heesterbeek, and Michael G. Roberts. The construction of next-generation matrices for compartmental epidemic models. *Journal of the Royal Society Interface*, 7(47):873–885, 2010.

[43] Pauline van den Driessche and James Watmough. Further notes on the basic reproduction number. *Mathematical Epidemiology*, 1945:159–178, 2008.

[44] Brian D. Hassard, Nicholas D. Kazarinoff, and Yieh-Hei Wan. *Theory and Applications of Hopf Bifurcation*, volume 41 of *London Mathematical Society Lecture Note Series*. Cambridge University Press, Cambridge, UK, 1981.

[45] Xihui Lin and Hao Wang. Stability analysis of delay differential equations with two discrete delays. *Canadian Applied Mathematics Quarterly*, 20(4):519–533, 2012.

[46] The MathWorks, Inc. *MATLAB Version 9.14.0 (R2023a)*. The MathWorks, Inc., Natick, MA, USA, 2023. Accessed: 2023-01-01.